Kinetics and Catalysis, Vol. 44, No. 5, 2003, pp. 692–700. Translated from Kinetika i Kataliz, Vol. 44, No. 5, 2003, pp. 755–763.

CATALYTIC REACTION MECHANISMS

Application of Statistical Lattice Models to the Analysis of Oscillatory and Autowave Processes in the Reaction of Carbon Monoxide Oxidation over Platinum and Palladium Surfaces

V. I. Elokhin, E. I. Latkin, A. V. Matveev, and V. V. Gorodetskii

Boreskov Institute of Catalysis, Siberian Division, Russian Academy of Sciences, Novosibirsk, 630090 Russia

Received November 4, 2002

Abstract—Statistical lattice models which imitate oscillatory and wave dynamics in the adsorbed layer during of carbon monoxide oxidation over Pt(100) and Pd(110) single crystals differing in the mechanism of autooscillation formation are compared. In the case of platinum, oscillations are due to phase transitions of the catalyst surface structure and surface reconstruction under the action of the reaction medium. In the case of palladium, the driving force of oscillations is phase transitions in the adsorbed layers on the catalyst surface, namely, the reversible formation of subsurface oxygen in the course of the reaction, which modifies the adsorption and catalytic properties of the surface. It is shown that, according to the proposed models, a change in the coverages ($CO_{ads} \longleftrightarrow O_{ads}$) in the autooscillation regimes occurs via the formation of a surface wave whose front is characterized by the high concentration of catalytically active sites that provide the maximal rate of CO_2 molecule formation. Under certain conditions, the formation of various spatiotemporal structures is observed in simulation experiments.

INTRODUCTION

It is known that catalytic reactions far from equilibrium may be accompanied by such unusual phenomena as oscillations, kinetic phase transitions, multiplicity of steady states, and chaos. Complex dynamic behavior of an isothermal reaction can be explained by the structure of the detailed reaction mechanism. Various mechanisms of oscillations have been found and studied which are associated with (1) surface structure transformation Pt(100)-*hex* $\longleftrightarrow$ Pt(100)-(1 × 1); (2) formation of surface oxides (Pd(110)); and (3) the "explosive" nature of interactions between adsorbed species. A common assumption in all these mechanisms is the spontaneous periodical transitions of metal from an inactive to highly active catalytic state. The method of photoelectron microscopy (PEEM) made it possible to discover in the early 1990s a new phenomenon: the formation of chemical waves on the surfaces of Pt and Pd single crystals under conditions of oscillation of the rate of chemical reactions. For instance, the regular propagation of the reaction fronts was observed for the reaction CO + O_2/Pt(110) with a spatial resolution of ~1 μm. These fronts were formed by O_{ads} and CO_{ads} adlayers [1].

A conventional approach to autooscillation modeling based on solving kinetic equations that reflect changes in the integral characteristics of the system, such as reaction rate and concentrations of surface substance, cannot explain at the microscopic level the formation of spatial–wave structures having the forms of solitons, spiral waves, and turbulence pattern under conditions of oscillations. Unlike this approach, imitation modeling based on the Monte Carlo methods makes it possible to describe the spatiotemporal dynamics of adsorbate distribution [2, 3] on real catalyst surfaces, whose structure may change under the action of the reaction medium. The goal of this work is to construct and study statistical lattice models that imitate oscillation and wave dynamics in the adsorbed layer in CO oxidation on the Pt(100) and Pd(110) surfaces, which differ in the mechanism of oscillation formation: (1) with structure transformation (Pt(100): (*hex*) $\longleftrightarrow$ (1 × 1)) and (2) with the formation of surface oxides (Pd(110)) [1].

MODEL DESCRIPTION

Pt(100). Experimental and theoretical studies show that the Pt(100) plane exhibits reversible surface structure transitions (*hex*) $\longleftrightarrow$ (1 × 1) under conditions of autooscillations. The activity of Pt in the (1 × 1) phase is due to the ease of O_2 molecule dissociation: the sticking coefficients $S_{(1\times1)} \approx 0.3$ is much greater than $S_{(hex)} \approx 10^{-3}$. The low activity of the hex phase is due to the low value of the sticking coefficient S_{O_2} and island growth in the course of CO adsorption preventing the dissociation of adsorbed oxygen molecules. It has been found that the spontaneous periodical transition of platinum from the low-active to highly active catalytic state, associated with the adsorbed CO-induced phase transition (*hex*) $\longleftrightarrow$ (1 × 1) of the Pt(100) plane, is a driving force of autooscillations. The detailed mechanism of the process is as follows [4]:

$$CO + * \longrightarrow CO_{ads}, \qquad \text{(I)}$$

0023-1584/03/4405-0692$25.00

$$CO_{ads}^{(hex)} \longrightarrow CO + *_{(hex)}, \quad \text{(II)}$$

$$(hex) \longrightarrow (1\times1)\text{: } 4CO_{ads} \longrightarrow 4CO_{ads}^{(1\times1)}, \quad \text{(III)}$$

$$(1\times1) \longrightarrow (hex)\text{: } *_{(1\times1)} \longrightarrow *_{(hex)}, \quad \text{(IV)}$$

$$O_2 + 2*_{1\times1} \longrightarrow 2O_{ads}^{(1\times1)}, \quad \text{(V)}$$

$$O_{ads}^{(1\times1)} + CO_{ads} \longrightarrow CO_2 + *_{(1\times1)} + *, \quad \text{(VI)}$$

$$CO_{ads}^{(1\times1)} \longrightarrow CO + *_{(1\times1)}, \quad \text{(VII)}$$

$$CO_{ads} + * \longrightarrow * + CO_{ads}, \quad \text{(VIII)}$$

where * is the active site on the surface ($*_{(1\times1)}$ or $*_{(hex)}$), step (VIII) reflects the mechanism of adsorbed CO diffusion via hops along a metal surface.

Pd(110). Compared to the Pt(100) plain, the clean Pd(110) surface does not restructure in the course of CO oxidation. Of the "oxide models" proposed for the explanation of oscillatory reaction dynamics, the most popular is the kinetic model with subsurface oxygen (O_{sub}) consisting of the conventional Langmuir–Hinshelwood mechanism and supplemented with the reversible step $O_{ads} \longleftrightarrow O_{sub}$. In this model, oscillations and surface waves are explained by purely kinetic reasons (changes in the catalytic and adsorption properties of the surface due to slow processes of formation and consumption of subsurface oxygen) and are not associated with the metal surface restructuring. The following sequence of oscillatory cycle has been proposed: (1) O_{sub} is only formed on the palladium surface covered with atomic oxygen O_{ads}, and this is accompanied by a decrease in the value of the sticking coefficient S_{O_2}; (2) the CO_{ads} layer is formed due to the fast reaction of adsorbed carbon monoxide molecules with adsorbed oxygen atoms O_{ads} with the formation of CO_2 molecules and their desorption; (3) the formation of vacant active sites in a high concentration, which is due to the reverse oxygen diffusion $O_{sub} \longrightarrow O_{ads}$ with the subsequent removal of O_{ads} in the reaction with CO_{ads} or due to slow reaction of O_{sub} with CO_{ads} to form CO_2; and (4) the transition to the initial oxygen layer proceeds from an increase in S_{O_2} because of a decrease in the concentration of O_{sub} ($\theta_{O_{sub}}$).

Based on our experiments using TPD, TPR, and XPS methods, the following detailed mechanism of the reaction was proposed [5, 6]:

$$O_{2(gas)} + 2* \longrightarrow 2O_{ads}, \quad \text{(I')}$$

$$CO_{gas} + * \longleftrightarrow CO_{ads}, \quad \text{(II')}$$

$$CO_{ads} + O_{ads} \longrightarrow CO_{2(gas)} + 2*, \quad \text{(III')}$$

$$CO_{ads} + * \longrightarrow * + CO_{ads}, \quad \text{(IV')}$$

$$O_{ads} + *_v \longrightarrow [*O_{sub}], \quad \text{(V')}$$

$$CO_{ads} + [*O_{sub}] \longrightarrow CO_{2(gas)} + 2* + *_v, \quad \text{(VI')}$$

$$CO_{gas} + [*O_{sub}] \longleftrightarrow [CO_{ads}*O_{sub}], \quad \text{(VII')}$$

$$[CO_{ads}*O_{sub}] + [*O_{sub}] \longrightarrow [*O_{sub}] + [CO_{ads}*O_{sub}], \quad \text{(VIII')}$$

$$CO_{ads} + [*O_{sub}] \longrightarrow * + [CO_{ads}*O_{sub}], \quad \text{(IX')}$$

$$[CO_{ads}*O_{sub}] \longrightarrow CO_{2(gas)} + * + *_v, \quad \text{(X')}$$

where $*$ and $*_v$ are the active sites on the surface and subsurface layers, respectively. The first step describes irreversible oxygen adsorption; the second step is the adsorption and desorption of CO. The third step corresponds to the reaction between CO_{ads} and oxygen atoms O_{ads}. The surface diffusion of CO_{ads} molecules and the formation of the layer of dissolved oxygen O_{sub} are represented by steps (IV') and (V'). The reaction between the CO_{ads} molecules and subsurface oxygen is described by step (VI'). The formation of a complex of CO_{ads} molecules on dissolved oxygen in the form $[CO_{ads}*O_{sub}]$ occurs both via the direct adsorption of CO from the gas phase (step VII'), and via CO diffusion along the surface (steps VIII' and IX'). The decomposition of the $[CO_{ads}*O_{sub}]$ complex is accompanied by the formation of CO_2 molecules and freeing adsorption sites $*$ and $*_v$ (step X').

In our modeling we used a squared $N \times N$ lattice (N = 400–1600) with periodical boundary conditions. The states of square cells were set according to the rules determined by the detailed mechanism of the reaction (e.g., in the case of Pd(110), each lattice cell can exist in one of five states: $*$, CO_{ads}, O_{ads}, $[*O_{sub}]$, and $[CO_{ads}*O_{sub}]$). The time was measured in terms of the so-called Monte Carlo steps (MC steps) consisting of $N \times N$ trials to choose and realize the main elementary processes. For a unit of time, each cell was called once in the average.

The probability of each step for the processes of adsorption, desorption, and reaction was determined by the ratio of the rate constant of a given step to the sum of the rate constants of all steps.

After each choice of one of the processes and an attempt to realize it, the program considered the internal diffusion cycle that involved M diffusion attempts for CO_{ads} molecules (usually M = 50–100). The reaction rate of CO oxidation and the surface coverages with reactants were calculated after each MC step as a ratio of the amount of CO_2 molecules formed (or the number of lattice cells in the corresponding state) to the overall amount of cells N^2 (the procedure was described in detail in [4, 5, 9]).

RESULTS AND DISCUSSION

For both mechanisms considered above, the appearance of oscillations in the CO oxidation rate was

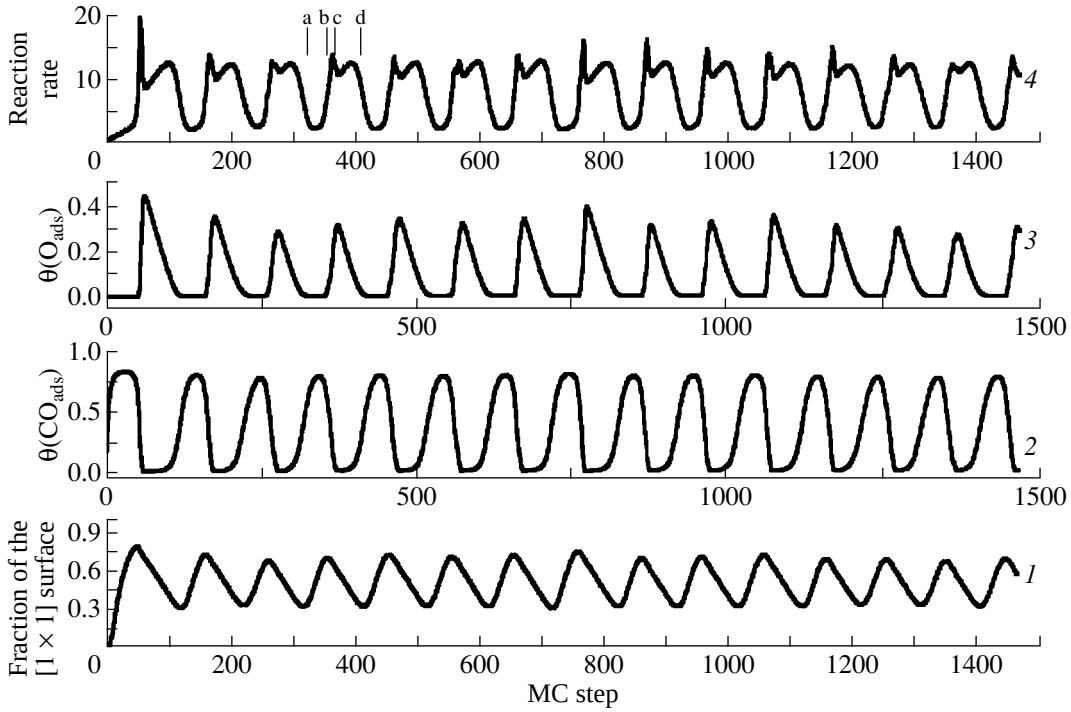

Fig. 1. Oscillations of the reaction rate and the surface coverage (θ) of Pt(100) for the lattice size $N = 384$ and the parameter $M = 100$. The values of the rate constants of elementary steps (Scheme 1): $k_1 = 2.94 \times 10^5$ ML s^{-1} $Torr^{-1}$ (1 ML = 9.4×10^{14} atom/cm^2), $P_{CO} = 5 \times 10^{-5}$ Torr, $k_2 = 4\ s^{-1}$, $k_3 = 3\ s^{-1}$, $k_4 = 2\ s^{-1}$, $k_5 = 5.6 \times 10^5$ ML s^{-1} $Torr^{-1}$, $P_{O_2} = 10^{-4}$ Torr.

observed in the narrow range of parameters, which are close to the experimental values [1, 7, 8].

CO oxidation on the Pt(100) surface. Figure 1 shows autooscillations of the rate of CO_2 formation, the surface coverage with O_{ads} and CO_{ads}, and the portion of the vacant surface in the (*hex*)- and (1×1) structures. At the initial moment, the platinum surface is in the (*hex*) state and only CO adsorption is allowed. Despite the low rate of (*hex*) $\longrightarrow$ (1×1) restructuring, the portion of the (1×1) rapidly grows. As a result of CO_{ads} diffusion, sites for oxygen adsorption are formed. However, the value of $O_{(1 \times 1)}$ coverage is very low due to the fast reaction with neighboring CO_{ads} molecules. When the maximal value of $\theta(CO_{ads}) \sim 0.8$ is attained, the adsorbed layer largely consists of $CO_{(hex)}$ and $CO_{(1 \times 1)}$ (Fig. 2a), which is accompanied by a sharp decrease in the reaction rate. Figure 2a' shows that the rate of CO_2 molecule formation in the CO_{ads} layer is low, but regions with a high concentration of vacant sites are available on the surface. In this regions, the $O_{(1 \times 1)}$ islands nucleate and propagate along the metal surface (Figs. 2b, 2c, 2b', 2c'). Figures 2b' and 2c show that the maximal intensity of CO_2 molecule formation is observed in the narrow zone at the boundary of the growing O_{ads} phase and the CO_{ads} layer. The appearance of such a narrow reaction zone when the surface coverage changes was experimentally observed by the field ion probe-hole microscopy technique with a resolution of ~5 Å [7]. Inside the oxygen island, the rate of CO_2 formation has an intermediate value; the lower value is in the CO_{ads} layer. The highest value of the reaction rate along the oscillation period corresponds to the moment when the perimeter of the reaction zone is maximum (Fig. 2c'). At the final stage of the oscillation cycle, the $\theta(CO_{ads})$ coverage increases due to CO molecule adsorption on the vacant sites (both (*hex*) and (1×1)) with the further transition of the (1×1) phase into (*hex*) (Figs. 2d, 2d').

A decrease in the parameter M to 50 does not affect the regular nature and uniformity of oscillations but leads to a small decrease in the period and amplitude of oscillations. However, with a decrease in M to 30, the period and amplitude of oscillations become irregular (Fig. 3). In this case, O_{ads} atoms are always present on the surface and mobile islands in the form of cellular structures, spiral fragments, etc., are formed (Fig. 4). Similar turbulent spatiotemporal structures were experimentally observed in the reaction of CO oxidation on Pt(100) using the methods of ellipsomicroscopy for surface imaging (EMSI) [8].

CO oxidation on Pd(110). In the whole range of parameters at which the reaction rate oscillated, the dependences of a change in the adsorbate concentration and the reaction rate have a similar nature (Fig. 5). A drastic increase in the reaction rate occurs simultaneously with the removal of the CO_{ads} layer and filling

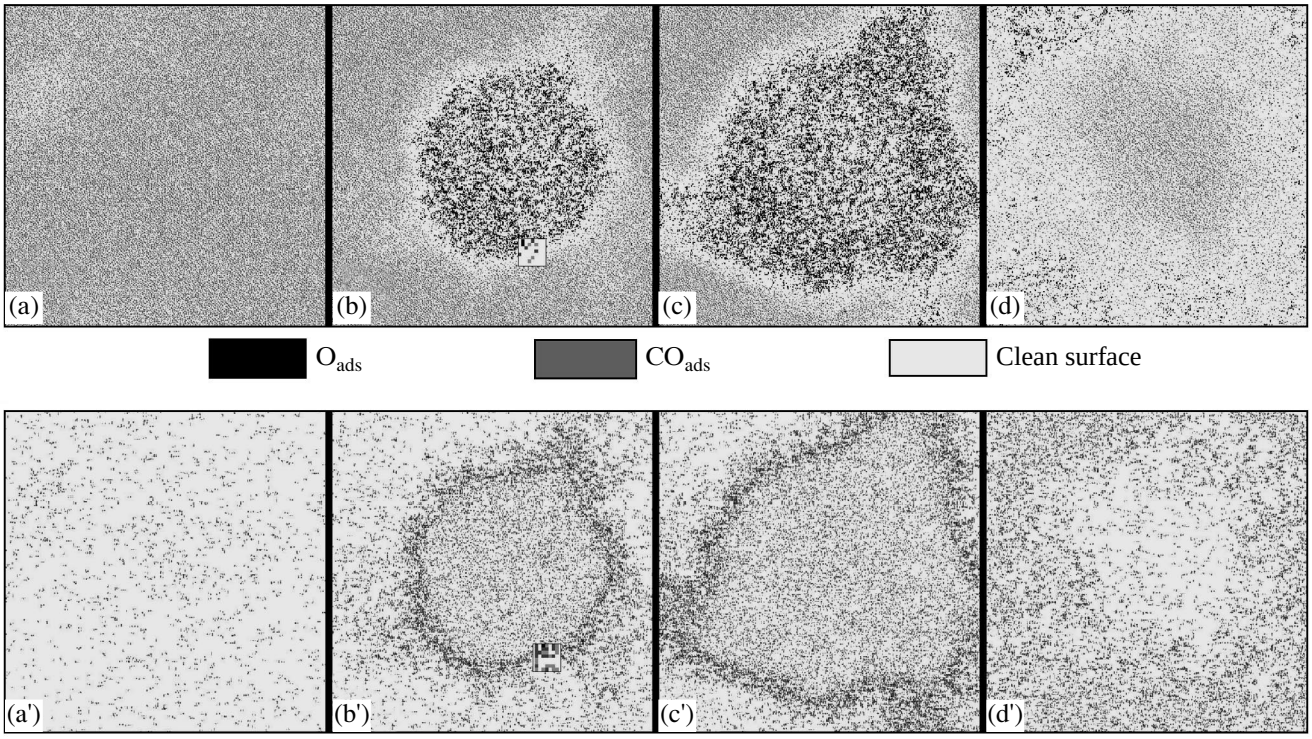

Fig. 2. The distribution of adsorbates over the surfaces (a–d) and the intensity of CO_2 formation (a'–d') at the moment when the surface coverage changes on Pt(100). The concentration of O_{ads} is shown in black, CO_{ads} is in grey, and free surface is in white. Parts a, a'–d, d' correspond to the moments 332, 360, 364, and 408 MC steps shown in Fig. 1, curve *4*.

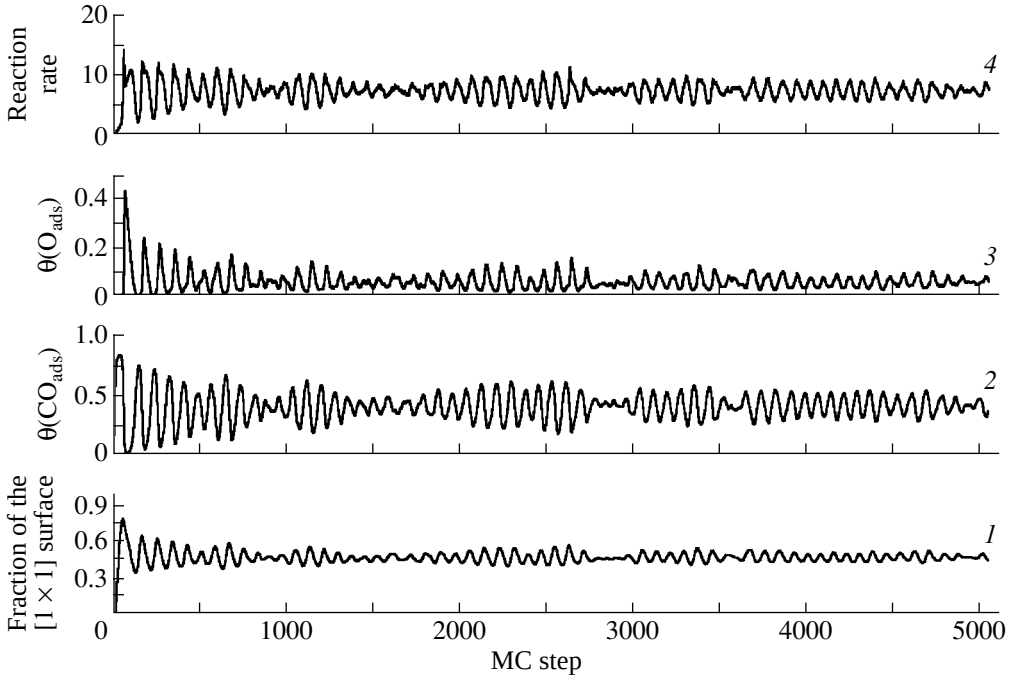

Fig. 3. Oscillations of the reaction rate and the surface coverage of Pt(100) for the lattice size $N = 384$ and the parameter $M = 30$.

the surface with the oxygen layer (Figs. 6a, 6d, 6a', 6d'). This moment of time on the curve of the concentration of subsurface oxygen corresponds to the minimal value for the given period. When the rate approaches its maximal value, the concentration of adsorbed oxygen redistributes: $O_{ads} \longrightarrow O_{sub}$. The position of the maximum on the curve of the concentration of subsurface oxygen determines the moment of a decrease in the reaction

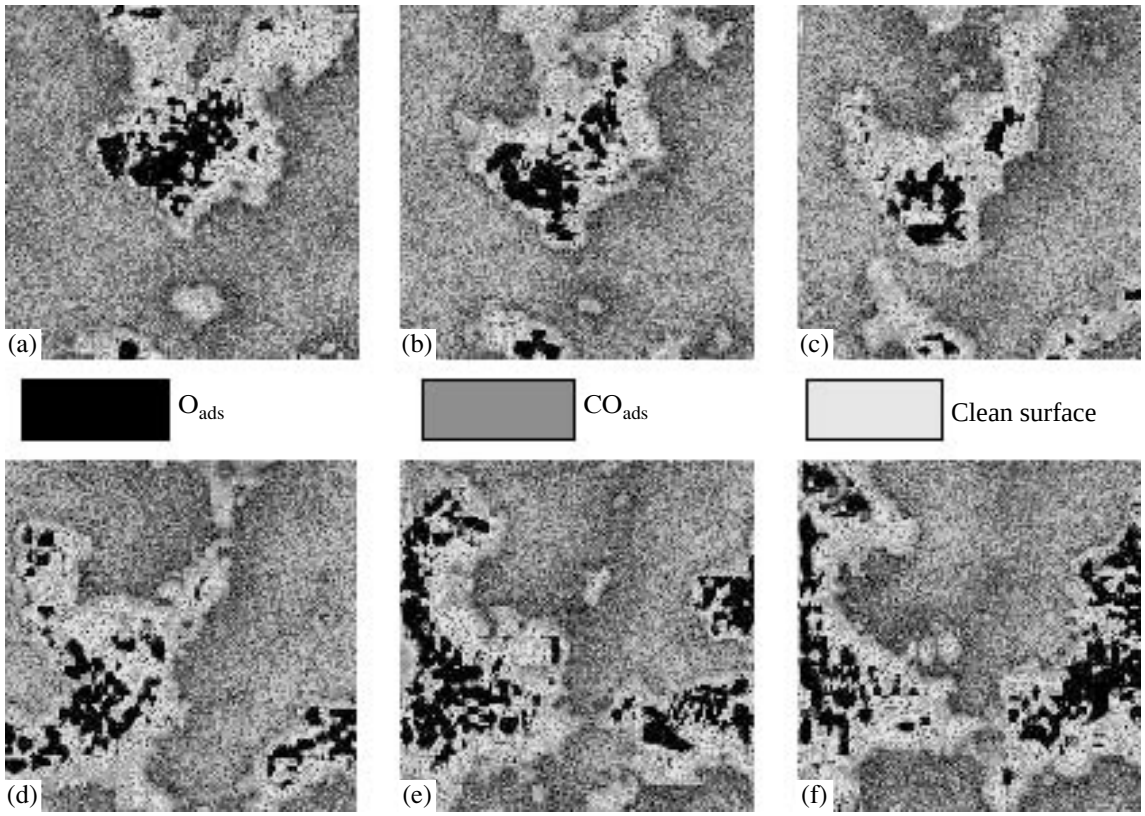

Fig. 4. The distribution of adsorbates over the surface in the case of the low rate of diffusion (M = 30). The concentration of O_{ads} is shown in black, CO_{ads} is in grey, and the free surface is shown in white.

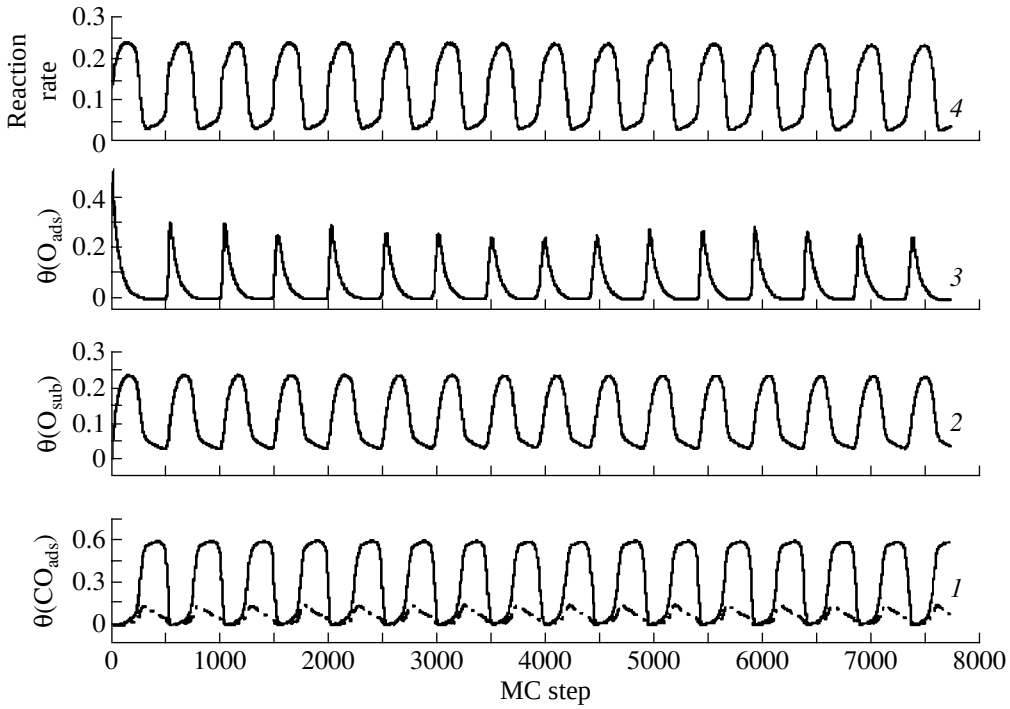

Fig. 5. Dynamics of changes in the coverages (θ) and the rate of CO oxidation on the Pd(110) surface: (*1*) [CO_{ads}∗O_{sub}] (dot-and-dash line), CO_{ads} (solid line), (*2*) [∗O_{sub}], (*3*) O_{ads}, and (*4*) the reaction rate; N = 768; M = 100. The values of the rate constants of steps (s^{-1}) (Scheme 2): $k_1 = 1$, $k_2 = 1$, $k_{-2} = 0.2$, k_3 = inf, $k_5 = 0.03$, $k_6 = 0.01$, $k_7 = 1$, $k_{-7} = 0.5$, and $k_{10} = 0.02$. The partial pressures of reagents (CO and O_2) and the concentrations of active sites on the palladium surface are included in the rate constants of adsorption k_1, k_2, and k_7.

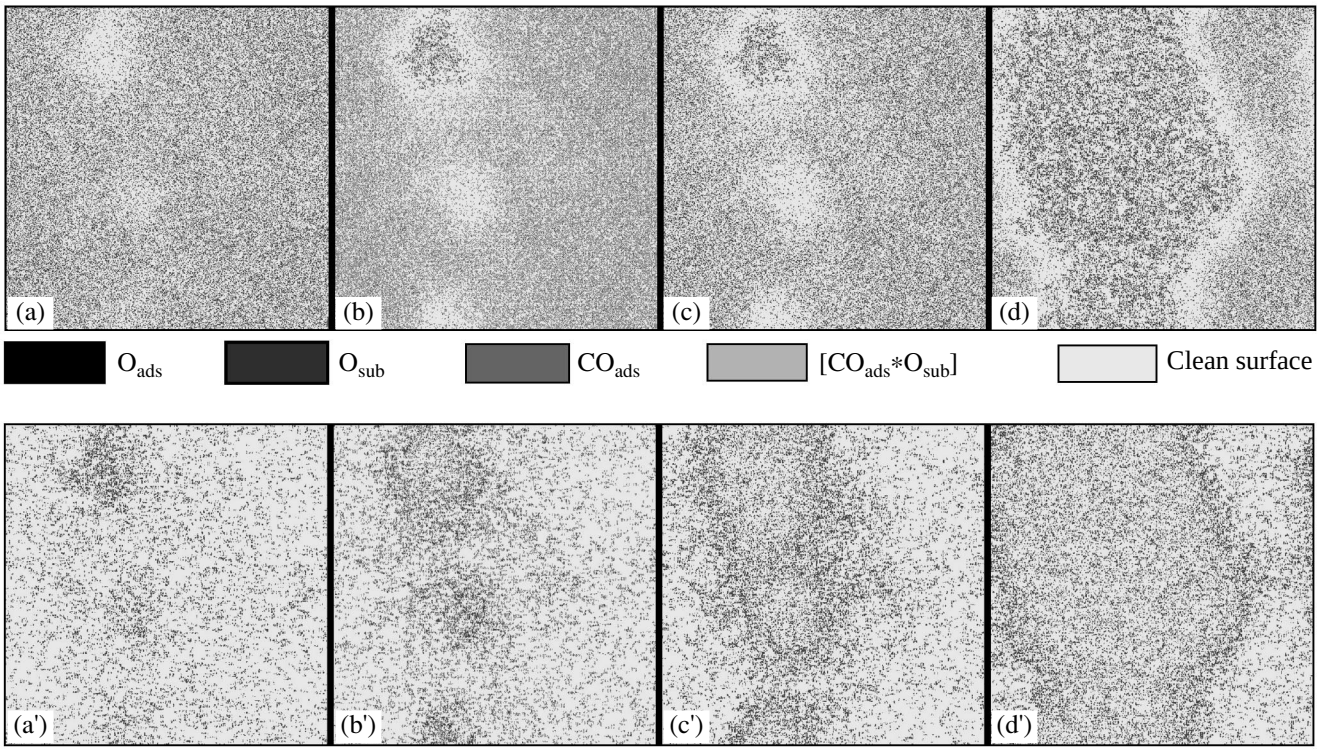

Fig. 6. The distribution of adsorbates over the surface (a–d) the intensity of CO_2 formation (a'–d') at the moment when the coverages on the Pd(110) surface.

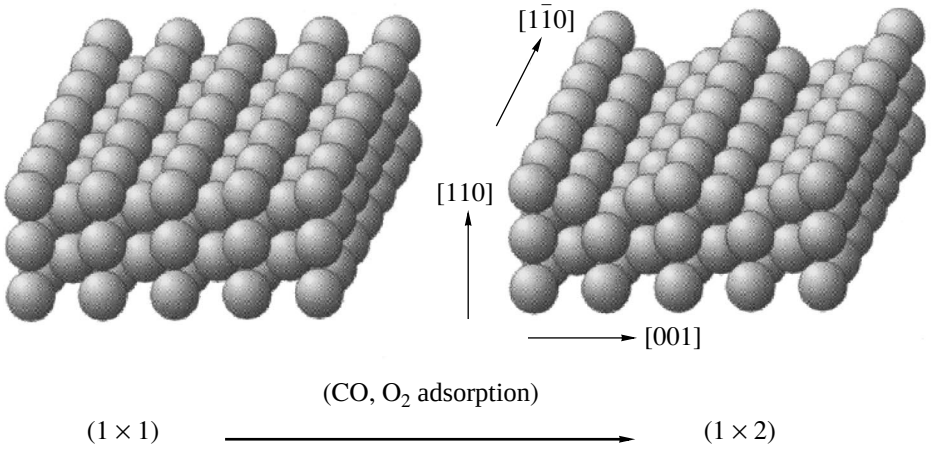

Fig. 7. The restructuring of the Pd(110)–(1 × 1) into (1 × 2) with missing/added rows in the course of O_2 or CO adsorption.

rate. Simultaneously, the surface accumulates CO_{ads}, and this process is accompanied by the complete removal of O_{ads}. The minimal value of the reaction rate is only stipulated by the interaction of CO_{ads} molecules with subsurface oxygen. A decrease in the concentration $\theta_{O_{sub}}$ to a certain critical value again creates favorable conditions for the reaction, and this completes the oscillation cycle. Changes in the coverages occur via the formation of the mobile wave, whose front is characterized by the high concentration of catalytically active sites responsible for the maximal rate of CO_2 molecule formation, as in the case of Pt(100).

A decrease in the parameter *M*, which determines the rate of CO_{ads} diffusion, leads, as in the case of Pt(100), to the chaotic nature of autooscillations and to the appearance of complex spatiotemporal structures on the surface.

It is known that CO adsorption or the dissociative adsorption of oxygen leads to the added/missing row

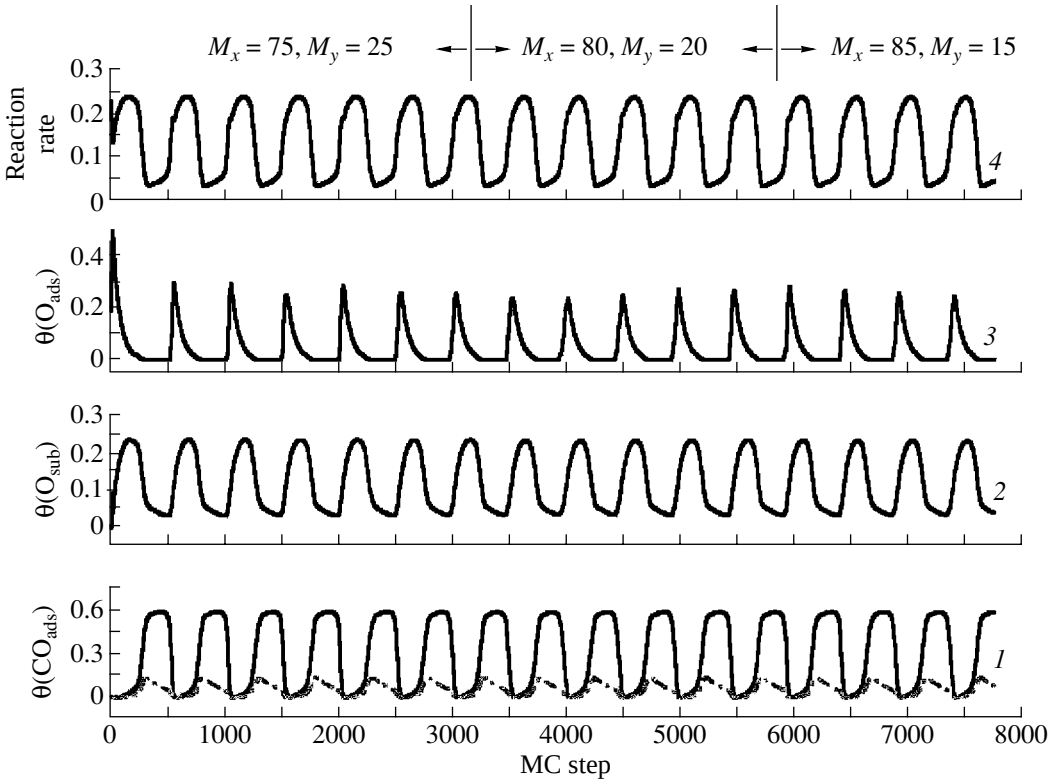

Fig. 8. The dynamics of changes in the coverages and the rate of CO oxidation on the Pd(110) surface at different ratios M_x/M_y: (*1*) $[CO_{ads}{*}O_{sub}]$ (dot-and-dash line), CO_{ads} (solid line), (*2*) $[O_{sub}]$, (*3*) O_{ads}, and (*4*) reaction rate.

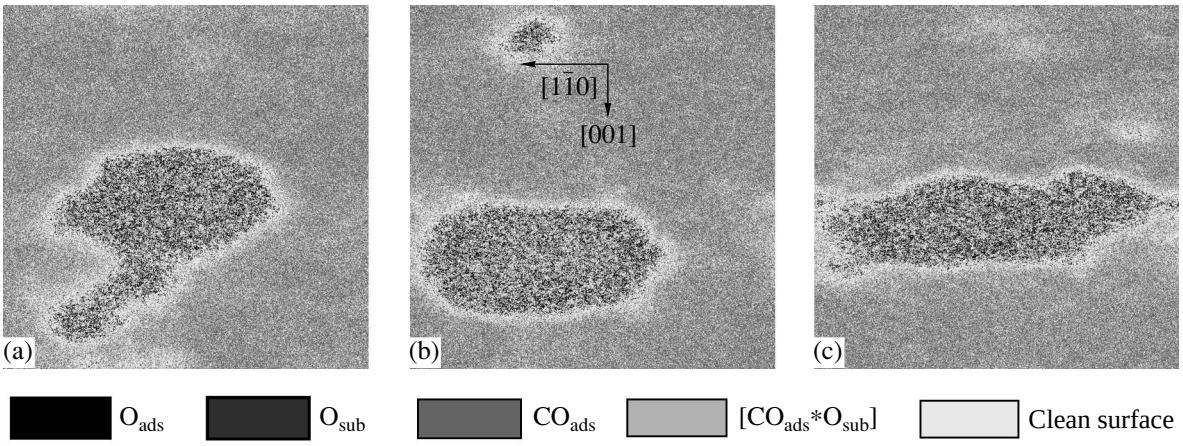

Fig. 9. The distribution of adsorbates over the surface in the course of oxygen wave propagation (N = 768, $\theta(O_{ads}) \approx 0.05$): (a) 2979 MC step, M_x/M_y = 75/25; (b) 3951 MC step, M_x/M_y = 80/20; (c) 7344 MC step, M_x/M_y = 85/15.

reconstruction of the Pd(110) plane $(1 \times 1) \longrightarrow (1 \times 2)$ (Fig. 7). As a result, the diffusion of CO_{ads} molecules along the rows of metal atoms occurs more rapidly than across the rows. We found that, if this effect is taken into account, such integral characteristics as the reaction rate and the values $\theta_{(CO)}$, $\theta_{(O)}$, and $\theta_{O_{sub}}$ do not change (Fig. 8). However, the propagation of a wave on the Pd(110)–(1×2) surface becomes noticeably anisotropic. Figure 9 shows the moments when coverages are changed. They correspond to approximately the same values of $\theta(O_{ads})$ and different M_x/M_y ratios (x and y are the directions of axes; the direction of the x axis coincides with the direction [1$\bar{1}$0]). It is seen that with an increase in M_x/M_y the mobile wave extends along the direction [1$\bar{1}$0].

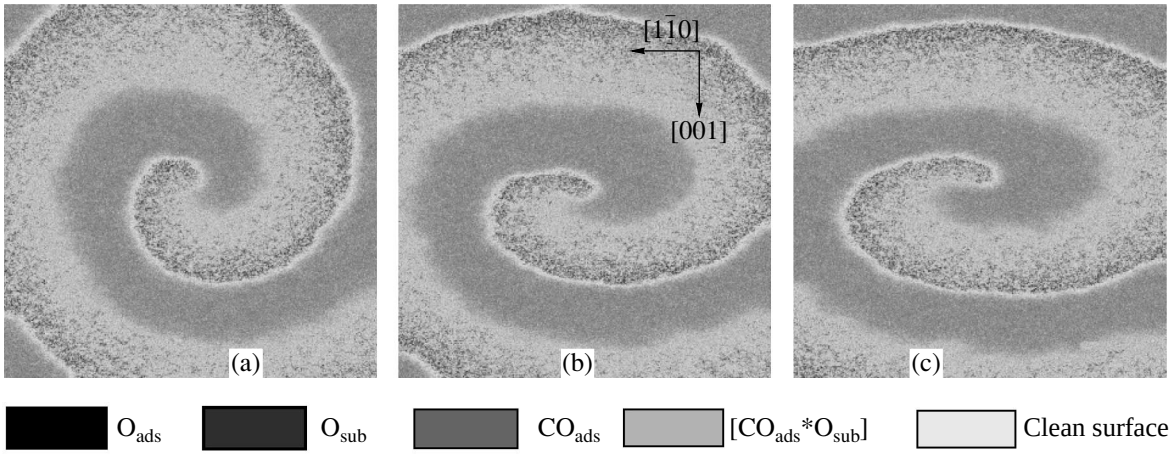

Fig. 10. Changes in the form of the spiral wave in the reaction of CO oxidation on the Pd(110) surface after the transition from the regime with isotropic diffusion (M_x/M_y = 50/50) to anisotropic (M_x/M_y = 80/20), N = 1536: (a) isotropic diffusion; (b) after the first turn of the spiral; and (c) after the second turn of the spiral.

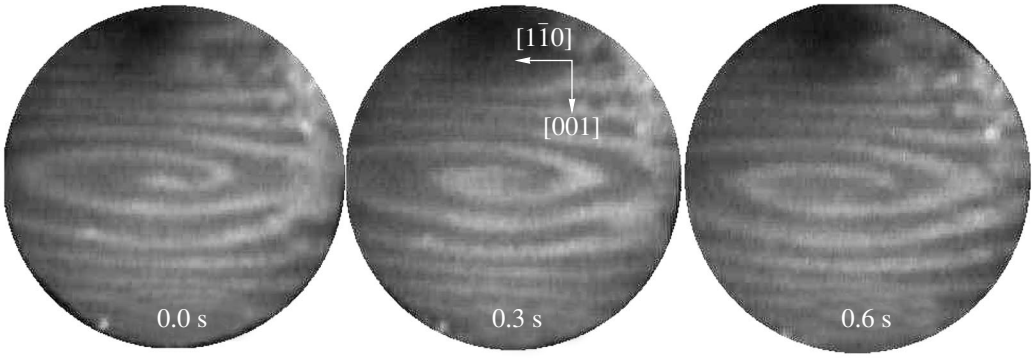

Fig. 11. PEEM images of the surface in the case of existence of a spiral wave in CO oxidation on Pd(110) [10]: $P_{O_2} = 4 \times 10^{-3}$ Torr, $P_{CO} = 1.6 \times 10^{-5}$ Torr, T = 349 K. Dark regions show CO_{ads}, light regions show O_{ads}; they corresponding to different values of work function.

The effect of anisotropy of CO_{ads} molecule diffusion becomes more apparent if one monitors the spatiotemporal structures, such as spiral waves, which are permanently present on the surface (detailed modeling of such structures was described in [9]). Figure 10 shows the evolution of modeled spiral waves after the transition from the isotropic regime (M_x/M_y = 50/50) to the anisotropic one (M_x/M_y = 80/20). Figure 10a shows the form of the spiral wave at the moment when the anisotropy of diffusion starts to work. Figures 10b and 10c show how spiral waves extend after passing through the first and second turns of the spiral. Such an asymmetric behavior of the spiral agrees very well with experimental data obtained using photoelectron emission microscopy (PEEM) [10]. Figure 11 shows images of the adsorbed layer in the case of the spiral wave in the reaction of CO oxidation on Pd(110). It is clearly seen that the spiral wave observed in the experiment [10] reflects the anisotropy of the single crystal Pd(110) surface in the direction [1$\bar{1}$0].

CONCLUSIONS

Thus, we constructed and studied statistical lattice models that describe the oscillation and wave dynamics in the adsorbed layer for the reaction of CO oxidation over Pt(100) and Pd(110) single crystal surfaces. These models differ in the mechanisms of formation of oscillations: a mechanism involving the phase transition of planes (Pt(100): (*hex*) $\longleftrightarrow$ (1 × 1)) and a mechanism with the formation of surface oxides (Pd(110)). The models demonstrate the oscillations of the rate of CO_2 formation and the concentrations of adsorbed reactants. These oscillations are accompanied by various wave processes on the lattice that models single crystalline surfaces. The effects of the size of the model lattice and the intensity of CO_{ads} diffusion on the synchronization and the form of oscillations and surface waves are studied. We showed the presence of a narrow zone of the reaction when the wave front propagates along the metal surface. This is supported by the results obtained by the methods of field electron microscopy (FEM) and field ion microscopy (FIM). We found that the inclusion

of CO_{ads} diffusion anisotropy, which reflects the real symmetry of the single crystal Pd(110) surface, does not affect the dynamics of oscillations of the integral characteristics of the reaction (the rate and the surface coverage), but it leads to the formation of ellipsoid spatiotemporal structures on the surface, which were observed experimentally with modern physical methods for surface science studies. It was shown that it is possible to obtain a wide spectrum of chemical waves (cellular and turbulent structures and spiral and ellipsoid waves) using the lattice models developed. These waves have been observed in experimental studies of oscillatory dynamics of catalytic reactions.

ACKNOWLEDGMENTS

This work was supported by the Russian Foundation for Basic Research (grant nos. 02-03-32568 and 03-03-89013) and by NWO (grant no. 47.015.002).

REFERENCES

1. Ertl, G., *Adv. Catal.*, 1990, vol. 37, p. 213.
2. Gelten, R.J., Jansen, A.P.J., van Santen, R.A., Lukkien, J.J., Segners, J.P.L., and Hilbers, P.A.J., *J. Chem. Phys.*, 1998, vol. 108, no. 14, p. 5921.
3. Zhdanov, V.P., *Surf. Sci. Rep.*, 2002, vol. 45, nos. 7–8, p. 233.
4. Latkin, E.I., Elokhin, V.I., and Gorodetskii, V.V., *J. Mol. Catal. A: Chem.*, 2001, vol. 166, p. 23.
5. Latkin, E.I., Elokhin, V.I., Matveev, A.V., and Gorodetskii, V.V., *J. Mol. Catal. A: Chem.*, 2000, vol. 158, p. 161.
6. Gorodetskii, V.V., Matveev, A.V., Kalinkin, A.V., and Niewenhuys, B.E., *Chemistry for Sustainable Development*, 2003, vol. 11, p. 67.
7. Gorodetskii, V.V. and Drachsel, W., *Appl. Catal., A*, 1999, vol. 188, p. 267.
8. Lauterbach, J., Bonilla, G., and Pletcher, T.D., *Chem. Eng. Sci.*, 1999, vol. 54, p. 4501.
9. Latkin, E.I., Elokhin, V.I., and Gorodetskii, V.V., *Chem. Eng. J.*, 2003, vol. 91, p. 123.
10. Block, J.H., Ehsasi, M., Gorodetskii, V., Karpowicz, A., and Berdau, M., *Stud. Surf. Sci. Catal.*, 1993, vol. 77, p. 189.